Electronic and vibrational properties of the As:InP(110) and Sb:InP(110) surfaces

H. M. Tütüncü[1] and G. P. Srivastava[2]
[1]*Sakarya Üniversitesi, Fen-Edebiyat Fakültesi, Fizik Bölümü, Adapazarı, Turkey*
[2]*Department of Physics, University of Exeter, Stocker Road, Exeter EX4 4QL, United Kingdom*
(Received 23 July 2001; published 27 December 2001)

We have investigated the atomic geometry, electronic structure, and vibrational properties of the As and Sb deposited InP(110)-(1×1) surface by using a combination of the plane-wave pseudopotential method and an adiabatic bond-charge method. For both adsorbates we have used the epitaxially continued layer structure. We have also used an exchange-reacted geometry for the adsorption of As. In general, our results agree well with available experimental measurements as well as recent *ab initio* calculations. It is found that the As:InP(110)-(1×1) and Sb:InP(110)-(1×1) systems are characterized by the presence of several phonon modes within the acoustic-optical band gap of bulk InP. The exchange-reacted geometry for As:InP(110) is further characterized by the presence of a clear gap of approximately 10 meV.

DOI: 10.1103/PhysRevB.65.035319 PACS number(s): 68.35.Ja, 73.20.At

I. INTRODUCTION

Considerable effort has been spent to investigate the atomic geometry[1–7] and electronic properties[8–12] of group-V covered III-V(110) surfaces, due to their scientific and technological importance. Room-temperature deposition of As, Sb, and Bi atoms on III-V(110) surfaces in general produces well-ordered interfaces, providing useful protypical systems to attempt extensive experimental and theoretical studies of their atomic geometry, electronic structure, and surface/interface phonon modes. The atomic structure of Sb:InP(110)(1×1) has been obtained by using low-energy electron diffraction[2–4] (LEED) and photoemission diffraction[7] (PED). On the theoretical side, this system has been studied by using a tight-binding total-energy scheme[13] and *ab initio* pseudopotential density-functional theory.[14–18] These experimental and theoretical techniques have confirmed that the Sb atoms are arranged in zigzag chains on the top of the valleys between In-P zigzag chains of the substrate, known as the epitaxially continued layer structure (ECLS). Room-temperature arsenic deposition on InP(110) is found to be poorly ordered, but a highly ordered phase is formed after annealing at temperatures above 300 °C. It is, therefore, useful to consider both the ECLS and an exchange-reacted structure (EXS) as proposed by Grossner, Santose, and co-workers.[19,20] The EXS consists of an InAs monolayer on the substrate surface.

In contrast to the numerous studies of the atomic geometry and electronic structure, studies of the vibrational properties of these surfaces are fewer and rather incomplete. It can be appreciated that studies of surface phonons are in general very important in view of their role in phase transition and relaxation processes of electronically or vibrationally excited states. Surface phonons for the ECLS of Sb:InP(110) were analyzed by Raman-scattering experiments.[21–24] This experimental technique has also been used to determine zone-center surface phonon modes on As:InP(110) using the EXS model. On the theoretical side, energies of zone-center phonon modes on the ECLS of Sb:InP(110) have been determined by using an *ab initio* approach for a restricted dynamical matrix.[16,17] Recently, Fritsch *et al.* have presented phonon-dispersion curves of the Sb:InP(110) surface using an *ab initio* linear-response formalism based on the density-functional scheme.[18] Zone-center phonon modes have been identified for the EXS model of As:InP(110) using an *ab initio* approach for a restricted dynamical matrix.[19] However, to our best knowledge, surface phonons for the ECLS model of As:InP(110) have not been studied yet.

In this paper we present results of *ab initio* pseudopotential studies of the atomic geometry and electronic states for the ECLS and EXS models for As:InP(110) and for the ECLS model for Sb:InP(110). These results are used in a bond-charge-model calculation of surface phonon dispersion and density of states. The calculated atomic geometry for these surfaces is in good agreement with experimental[4,7] and previous theoretical results.[16–19] For the ECLS models of As:InP(110) and Sb:InP(110) we compare and contrast our results with a previous first-principles calculation[19,18] and Raman-scattering experiment.[22,19] We also provide a detailed discussion of the similarities and dissimilarities in the phonon spectra for As:InP(110) and Sb:InP(110).

II. METHOD

We have used the local-density approximation (LDA) of the density-functional theory, with Ceperley-Alder correlation functional[25] and *ab initio* pseudopotentials,[26] to determine the relaxed atomic geometry and electronic structure of the systems under study. We considered an artificially constructed periodic geometry along the surface normal direction. The span of a unit cell along the surface normal was equivalent to 18 atomic layers, which included an atomic slab and a vacuum region. For the ECLS model, the atomic slab consisted of nine substrate layers (InP) and two group-V–group-V layers. For the EXS model, the P atoms in the top and bottom layers were replaced with As atoms. The electronic wave functions were expanded in terms of a basis set of plane waves, up to a kinetic-energy cutoff of 12 Ry, and the Kohn-Sham equation was solved using an iterative conjugate gradient scheme to find the total energy and atomic forces. The atoms were then moved towards their

optimum configuration following a conjugate gradient algorithm.[27]

The adiabatic bond-charge model (BCM) has proved to be a reliable and physically grounded dynamical model for the study of the lattice dynamics of III-V semiconductors.[28–30] The main concept in the BCM is that the valence electron charge-density distribution is represented by massless bond charges (BC's), endowed with translational degrees of freedom. For bulk materials, each III-V bond is replaced by a charge Ze which is placed towards anion, dividing a bond in the ratio 3:5. Each of the cations and anions is assigned a charge of -2Ze. The interactions included in the BCM are the Coulomb interaction between all particles (ion-ion, ion-BC, and BC-BC), a central short-range interaction between nearest-neighbor particles, and a bond-bending interaction involving the BC-ion-BC angle.[29] The bond-bending potential is given as

$$V_{bb}^{(\Delta)}=\frac{1}{2}B_{\Delta}(\mathbf{r}_{\Delta i}\cdot\mathbf{r}_{\Delta j}+a_{\Delta}^{2})^{2}/4a_{\Delta}^{2}, \tag{1}$$

where $\mathbf{r}_{\Delta k}$ is the distance vector between the ion type Δ and its neighboring bond-charge k, a_{Δ}^{2} is the equilibrium value of $|\mathbf{r}_{\Delta i}\cdot\mathbf{r}_{\Delta j}|$, and B_{Δ} is the bond-bending force constant.

For the present investigations, we applied the BCM within a repeated slab scheme.[31,32] For the EXS geometrical model the supercell contained 22 ions (11 In, 9 P, and 2 As) and 44 BC's located in a slab of 11 atomic layers, and a vacuum region consisting of nine layers of InP. For the ECLS geometrical model, the supercell contained 22 ions including nine In, nine P, and four group-V atoms, and 46 BC's. In order to maintain overall charge neutrality within the ECLS supercell, each BC was assigned a charge Ze and each ion in the adsorbate layer was assigned a charge of -2.5Ze. The BCM interaction parameters were essentially those used for bulk InP,[29] except for the following considerations.

Atoms in the top three layers on each side of a supercell were placed in their relaxed positions, obtained from the pseudopotential calculations described above, while deeper lying atoms were taken at their bulk positions. The positions of the dangling BC's were determined from the maximum valence electron density obtained from the pseudopotential calculations [see Fig. 2(b)], as discussed later. Since ionic environments in the bulk and at the surfaces are different, the force constants for the bulk and surface geometries will also be different. Thus for the surface calculations the second derivatives of the central ion-ion and ion-BC potentials (ϕ'') are scaled[33,34] as

$$\phi''_{\text{surface}}=\frac{r_{\text{bulk}}^{2}}{r_{\text{surface}}^{2}}\phi''_{\text{bulk}}, \tag{2}$$

where r_{bulk} and r_{surface} denote the magnitude of the interparticle distance (ion-ion, ion-BC, and BC-BC) for bulk and surface, respectively. Although the bond-bending force-constant parameters B_1 and B_2 are taken as their bulk values, the elements of the short-range bond-bending ion-BC matrices between the top-layer atoms and their neighboring BC's

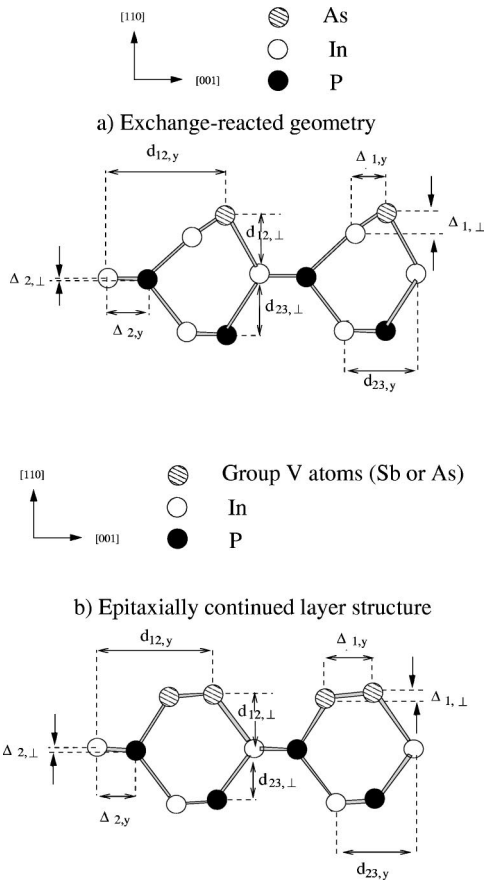

FIG. 1. Schematic relaxed side view of III-V(110). (a) An exchange-reacted structure and (b) the epitaxially continued layer structure.

TABLE I. Calculated structural parameters for exchange-reacted and epitaxial continued layer structures for As on the InP(110) surface. Distances are in Å.

Exchange-reacted geometry for As on InP(110)									
	$\Delta_{1,\perp}$	$\Delta_{2,\perp}$	$\Delta_{1,y}$	$\Delta_{2,y}$	$d_{12,\perp}$	$d_{23,\perp}$	$d_{12,y}$	$d_{23,y}$	ω_1
Present	0.78	0.11	1.23	1.41	2.26	2.10	4.45	2.88	32.38°
ab initio[a]	0.80	0.15	1.24	1.42	2.25	2.14	4.48	2.87	32.82°
Epitaxial continued layer structure for As on InP(110)									
	$\Delta_{1,\perp}$	$\Delta_{2,\perp}$	$\Delta_{1,y}$	$\Delta_{2,y}$	$d_{12,\perp}$	$d_{23,\perp}$	$d_{12,y}$	$d_{23,y}$	ω_1
Present	0.09	0.04	1.59	1.48	2.09	2.03	4.20	2.87	3.24°
ab initio[a]	0.11	0.06	1.59	1.50	2.10	2.07	4.15	2.75	3.96°
Epitaxial continued layer structure for Sb on InP(110)									
	$\Delta_{1,\perp}$	$\Delta_{2,\perp}$	$\Delta_{1,y}$	$\Delta_{2,y}$	$d_{12,\perp}$	$d_{23,\perp}$	$d_{12,y}$	$d_{23,y}$	ω_1
Present	0.12	0.07	1.97	1.43	2.42	1.96	4.45	2.88	3.48°
PED[b]	0.13		1.87		2.41		4.59		3.97°
ab initio[c]	0.16	0.07	1.98	1.46	2.44		4.44		4.62°
ab initio[d]	0.20	0.10	1.96	1.52	2.43		4.47		5.82°

[a]Reference 19.
[b]Reference 7.
[c]Reference 17.
[d]Reference 18.

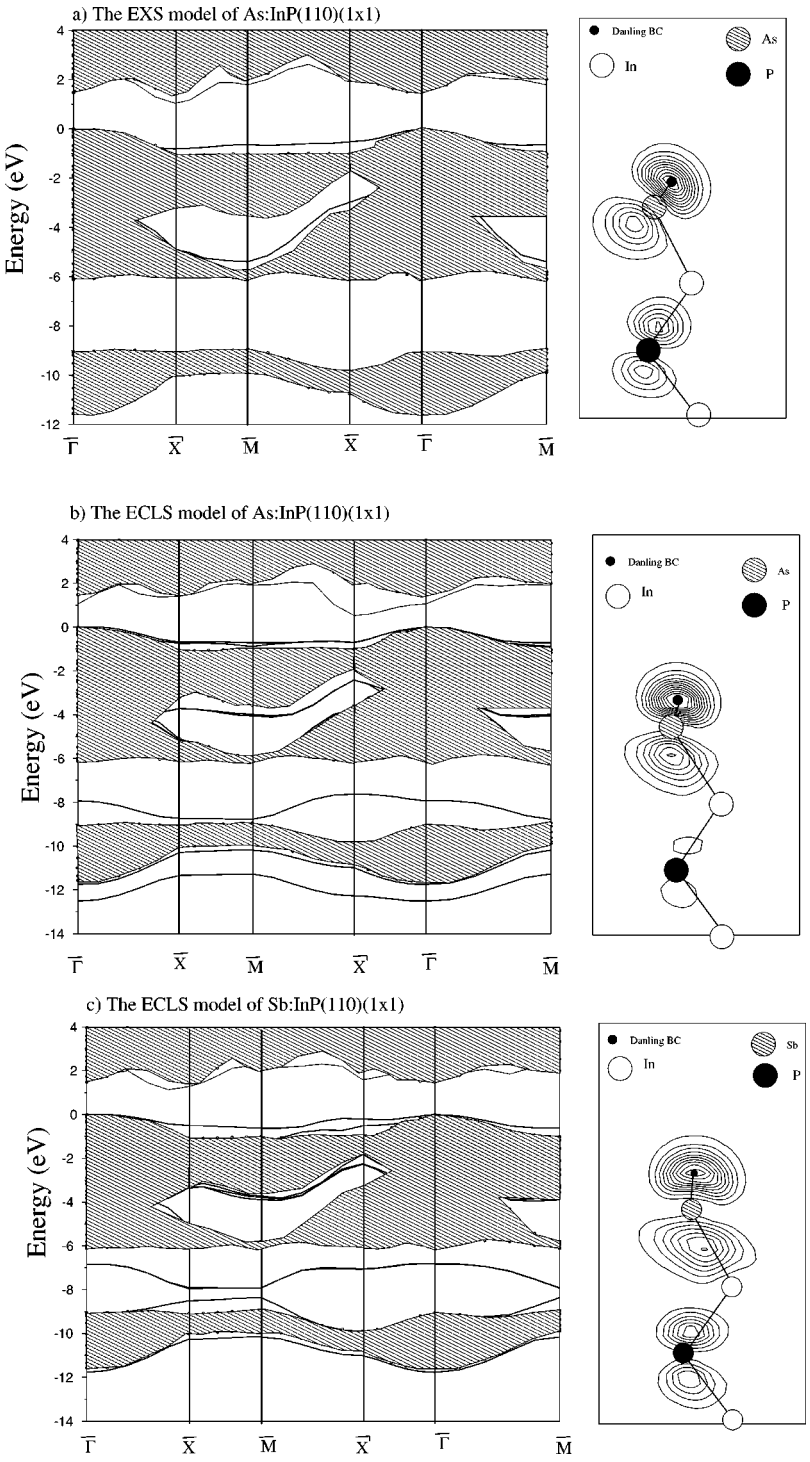

FIG. 2. Electronic band structure and charge density of the highest occupied state for the (a) exchange reacted geometry of As:InP(110), (b) epitaxially continued layer structure of As:InP(110), and (c) epitaxially continued layer structure of Sb:InP(110).

generally become very different from their bulk values because the dot product $\mathbf{r}_{\Delta i} \cdot \mathbf{r}_{\Delta j}$ for neighboring BC's changes considerably on the relaxed surface.

III. RESULTS

A. Atomic geometry and electronic structure

Our theoretical lattice constant for bulk InP is 5.67 Å, and this value has been used in the surface calculations. The calculated structural parameters for the surface geometries considered in Fig. 1 are given in Table I. It can be seen that the atomic relaxation on the exchange-reacted geometry of As:InP(110) has a similar pattern to that of the clean InP(110) surface: the surface-layer As atoms move out of the surface whereas the surface-layer In atoms move inside the surface. As expected, our predicted structural parameters are in remarkable agreement with a recent *ab initio* calculation.[19] Agreement between our results and the experimental[7] and other theoretical results[17,18] is also good for the ECLS. Since the In-As, In-Sb, As-P, and Sb-P bonds are partially ionic, the first-layer chain might be tilted. However, the tilt angle of the

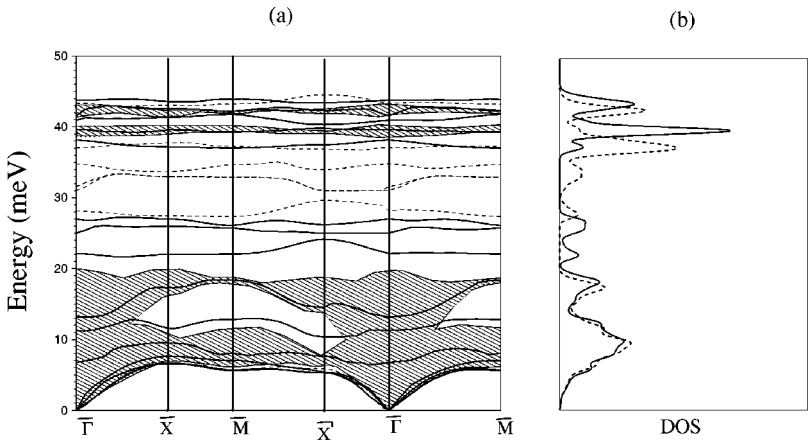

FIG. 3. (a) Surface phonon-dispersion curves for the exchange-reacted geometry of As:InP(110). The results for the clean InP(110) surface are shown by dashed lines. Hatched region shows projection of bulk phonon states. (b) Phonon density of states for the corresponding surfaces.

V-V chain is very much smaller than that of the clean InP(110) surface, due to the chain atoms being isoelectronic and having a sufficient number of electrons to fill all dangling bonds. The tilt angle of the As-As chain is determined to be 3.2° while it is found to be 3.5° for the Sb-Sb chain. For the ECLS geometry of As:InP(110), the In-As, P-As, and As-As bond lengths are determined as 2.54 Å, 2.35 Å, and 2.55 Å, respectively. These values are similar to those reported in the work of Grossner *et al.*[19] at 2.55 Å, 2.35 Å, and 2.56 Å, respectively. For Sb/InP, the Sb-Sb bond length is obtained to be 2.81 Å, which is in good agreement with the sums of the covalent radii, $r_{Sb}+r_{Sb}=2.80$ Å. Our calculated In-Sb and P-Sb bond lengths are found to be 2.71 Å and 2.55 Å, respectively, which were measured as 2.80 Å and 2.52 Å by LEED experiments.[4]

The electronic band structure for the exchange-reacted geometry, displayed in Fig. 2(a), shows two occupied surface bands and the lowest unoccupied band. The highest occupied state is made of the dangling bond sp^3-like orbital of the surface As atoms and also has a similar but small contribution from the third-layer P atoms. The electronic band structures for As:InP(110) and Sb:InP(110) with the ECLS termination are presented in Figs. 2(b) and 2(c), respectively. In the energy range spanning the ionic gap and slightly below the bulk valence-band continuum, there are two bands which are derived from the *s* orbitals of the overlayer atoms and they show strong dispersion along the chain direction (i.e., they show quasi-one-dimensional dispersion along $\bar{\Gamma}$-$\bar{X}$ and $\bar{X}'$-$\bar{M}$). As can be seen from Fig. 2, the highest occupied surface state is primarily made of the p_z orbitals from the overlayer atoms, but also has some contribution from the substrate atoms.[15]

Our calculated electronic structures for the ECLS and EXS models are generally similar to those obtained in the work by Grossner *et al.*[19] Small differences between the two sets of results are typical of such calculations, but lie within the limits of the accuracy in pseudopotential-LDA calculations of surface states. In the present case, such small differences could have originated from differences in the details of computational schemes, including the use of different kinetic-energy cutoffs (12 Ry in this work and 15 Ry in the work by Grossner). Even with the use of the same computational tools, slightly different results have been obtained for the same system (see, for example, results for Sb:InP(110) by Srivastava[15] and Schmidt *et al.*[35]).

It is interesting to remark that within the routinely available range of angle-resolved photoemission (ARPE) data for surface systems, i.e., within a binding energy range of 3 eV or so, the surface band structure of both the EXS and ECLS geometries for As:InP(110) are rather similar. This would make it difficult to distinguish between the two structural models based on energy dispersion obtained from ARPE experiments. In this respect surface phonon spectroscopies might prove more useful, as we discuss in the next two subsections.

B. Surface phonons

For the overlayer systems studied here, we have identified, as expected, up to a total of twelve surface modes corresponding to vibrations of atoms in the top two layers. Three of these are surface acoustic modes, and the rest are surface optical modes. The surface acoustic modes may appear as truly localized by falling below the bulk continuum at the edges of the surface Brillouin zone. Surface optical

TABLE II. Selected surface phonon frequencies (in meV) of As:InP(110) for the exchange-reacted geometry at the $\bar{\Gamma}$ point and their comparison with a recent *ab initio* phonon calculation and Raman-scattering experiment.

Source	A'' modes				A' modes			
Present	6.7	25.0	39.6	13.1	22.1	27.0	38.2	44.3
ab initio[a]	(5.9 and 8.3)				24.3	27.5		
Raman scattering[a]	(5.6 and 7.4)							

[a]Reference 19.

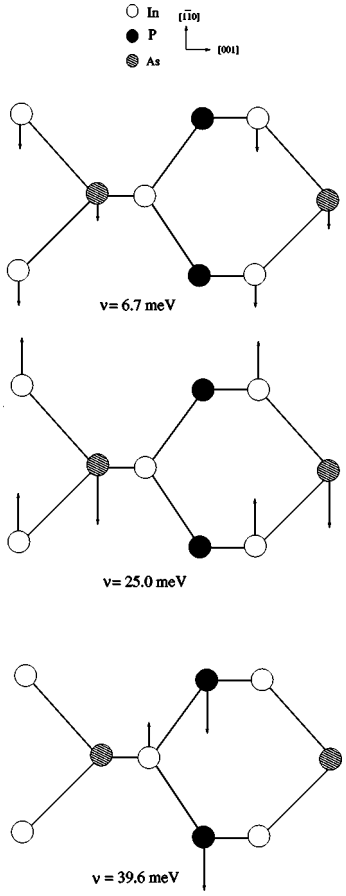

FIG. 4. The atomic displacement patterns of A'' phonon modes for the exchange-reacted geometry of As:InP(110) at the zone center.

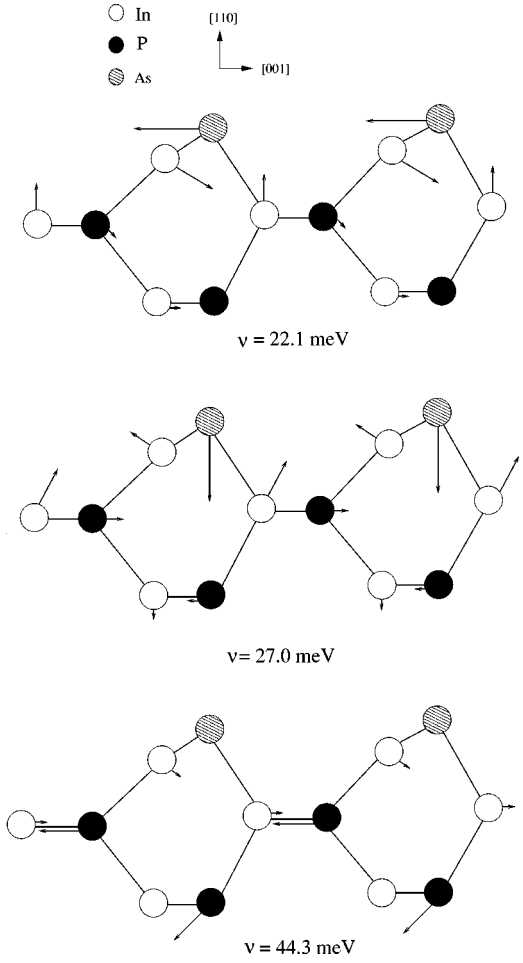

FIG. 5. The atomic displacement patterns of A' phonon modes for the exchange-reacted geometry of As:InP(110) at the zone center.

modes may appear as truly localized both within the acoustic-optical gap region and above the optical continuum of the bulk InP spectrum.

In our bulk calculations, the energy of longitudinal acoustic (LA) phonon mode (20 meV) at the X point of the bulk Brillouin zone is 3 meV lower than the experimentally measured value of 23 meV.[36] Thus our work slightly overestimates the gap between the acoustic and optical modes of the bulk of InP. We will keep this in mind when discussing any localized modes that are found in the energy range 20–23 meV.

In order to discuss polarization of surface modes it is helpful to note that, according to the irreducible representations of the point-group symmetry of the atomic slab in the supercell (C_s or m), surface phonon modes along the $\bar{\Gamma}$-$\bar{X}'$ direction are labeled as A'' if atomic vibrations are along the surface-atomic zigzag chain (i.e., along $[1\bar{1}0]$), and as A' if vibrations are in the sagittal plane defined by the [001] and [110] directions.

1. As:InP(110) with EXS termination

The phonon-dispersion curves for the EXS termination of the As:InP(110) surfaces are shown in Fig. 3(a). For comparison, we have shown the results for the clean InP(110) surface by dashed lines. For both the adsorbate covered and the clean surface, four phonon states appear in the acoustic-optical (ac-op) gap range. We find that the highest surface optical-phonon branch lies at energies similar to that on the clean surface. Figure 3(b) presents the phonon density of states for As:InP(110) together with the phonon density states for clean InP(110). Adsorption of As gives rise to two clear peaks at 22 and 27 meV. The second peak clearly corresponds to localized gap phonon modes, while the first peak may possibly be a resonant peak as it lies close to the top of the bulk acoustic continuum.

The calculated zone-center phonon modes for the EXS geometry are listed in Table II. These are compared with a recent *ab initio* calculation and Raman-scattering experiment.[19] Figure 4 illustrates the displacement patterns of some of the A'' phonon modes at the zone center. A Raman-scattering experiment[19] yields two A'' modes at energies of 5.9 meV and 8.3 meV in the bulk acoustic region of InP. The presently calculated A'' phonon mode at 6.7, at nearly the average value of the Raman-scattering A'' phonon modes, is a resonance state which includes a large contribution from the In atoms in the third and fourth layers. The second A'' phonon mode at 25.0 meV is a chain mode, consisting of opposing vibrations of the first-layer In and As atoms in the zigzag chain direction. The highest A'' phonon

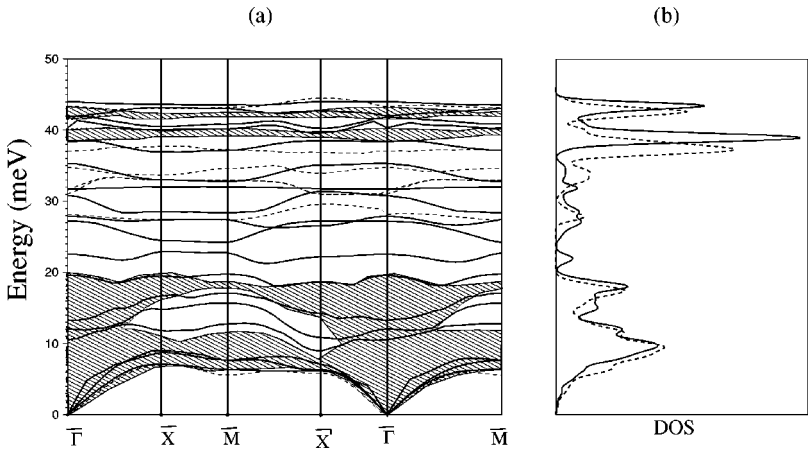

FIG. 6. (a) Phonon-dispersion curves for the epitaxially continued layer structure of As:InP(110). The results for the clean InP(110) surface are shown by dashed lines. (b) The corresponding phonon density-of-states curves.

mode at 39.6 meV results from the motion of the second-layer atoms, but atomic vibrations in the first layer are negligible. The vibrational patterns of A' phonon modes are displayed in Fig 5. The phonon mode at 22.1 meV can be compared with the phonon mode at 24.3 meV in the *ab initio* phonon calculation of Grossner, Schmidt, and Bechstedt.[19] This phonon mode includes a bond-stretching character due to opposing motion of In and As atoms in the [001] direction. We obtain a gap phonon mode at 27.0 meV with opposing vibrations of As and In atoms in the surface normal direction. This phonon mode compares very well with the phonon mode at 27.5 meV in the recent *ab initio* phonon calculation.[19] Although the mass of the As atom is nearly 2.4 times bigger than that of the P atom, the energy location of the highest surface optical-phonon mode for As:InP(110) is similar to that for clean InP(110). This feature can be readily explained by noting that this phonon mode arises due to opposing vibrations of the second-layer atoms in the [001] direction. In addition to this, this phonon mode also includes a large atomic vibration from the third-layer P atoms.

2. As:InP(110) with ECLS termination

The surface phonon dispersion and the density of states for the ECLS termination of As:InP(110) are presented in Figs. 6(a) and 6(b), respectively. Seven surface-localized phonon states are found to appear in the ac-op gap region. Once again, for comparison the corresponding results for the clean surface are shown by dashed lines in Figs. 6(a) and 6(b).

The displacement patterns of A'' phonon modes at the $\bar{\Gamma}$ point are displayed in Fig. 7. The surface optical-phonon mode at 14.0 meV is pictured by the chain layer vibrating against the second layer. Adsorption of As leads to the gap A'' phonon modes at 27.2 and 31.7 meV. The former is the As-As chain mode, totally localized within the adsorbate layer, and it has a displacement pattern similar to the phonon mode at 25.0 meV for the EXS geometry. The difference in the energies of this mode for the two geometries can be explained in terms of the mass difference between In and As atoms. The second gap A'' phonon mode at 31.7 meV for the

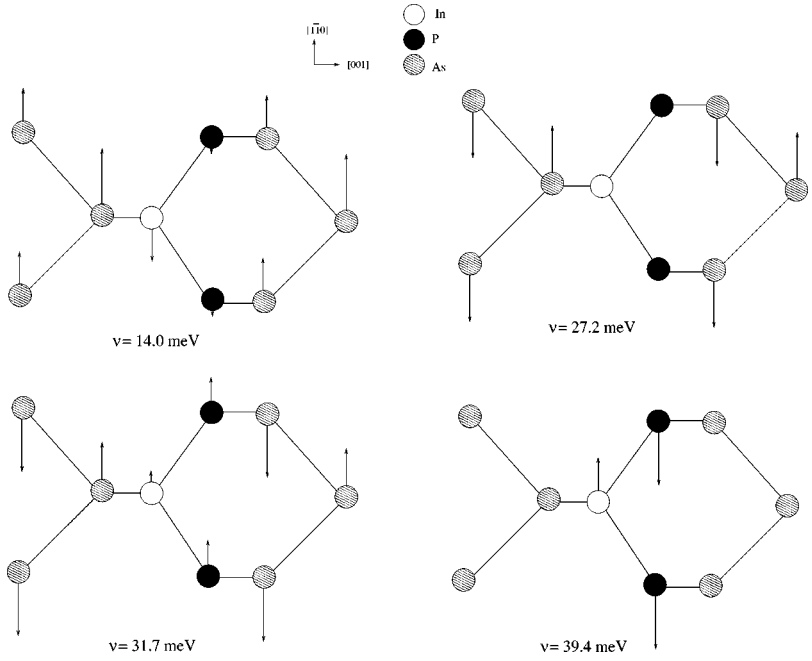

FIG. 7. The atomic displacement patterns of A'' phonon modes for the epitaxially continued layer structure of As:InP(110) at the zone center.

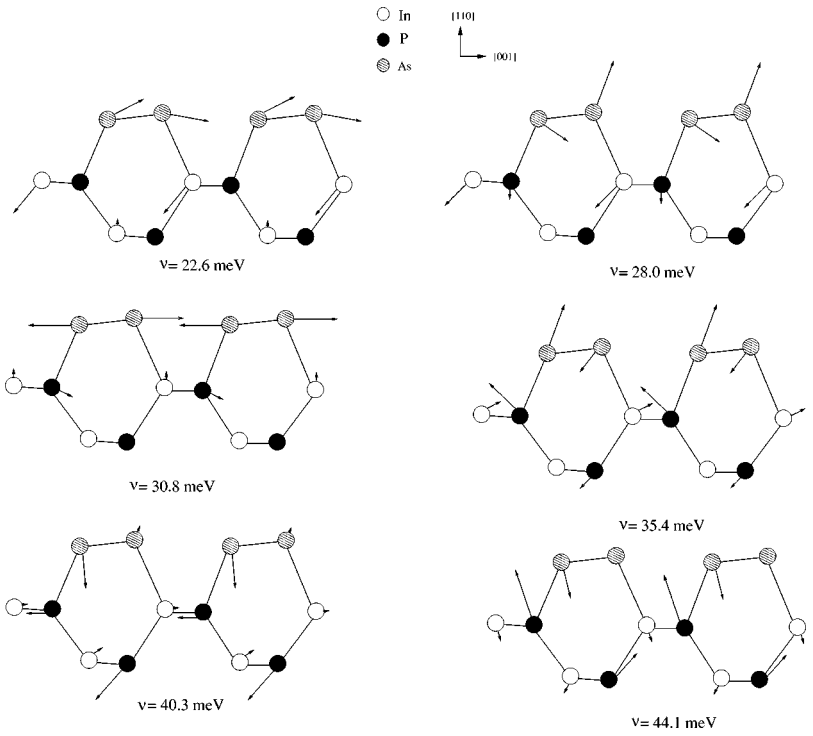

FIG. 8. The atomic displacement patterns of A' phonon modes for the epitaxially continued layer structure of As:InP(110) at the zone center.

ECLS geometry includes also large atomic vibrations from the second- and third-layer P atoms. As can be seen from Fig. 7, the highest A'' is localized to the subsurface layer for this structure too.

We obtain six A' phonon modes (see Fig. 8) at energies 22.6, 28.0, 30.8, 35.4, 40.3, and 44.1 meV. The first one is due to vibrations of first-layer As atoms and subsurface-layer In atoms. The phonon mode at 28.0, 30.8, and 35.4 meV are truly localized gap phonon modes, as these lie well inside the ac-op gap region. The first of these includes a rotational character due to opposing motion of surface-layer atoms in the surface normal direction, while the second corresponds to the As-As bond stretching. We note that the In-P bond-stretching mode has been identified at 28.1 meV for the clean InP(110) surface.[31] With increased phonon energies, atomic vibrations of the second- and third-layer P atoms become very important due to the large mass difference between P and anion atoms (As or In). This can be seen for the phonon modes at 35.4, 40.3, and 44.1 meV, all of which include larger atomic vibrations from the second- and third-layer P atoms.

3. Sb:InP(110) with ECLS termination

Figures 9(a) and 9(b) show the calculated surface phonon dispersion and density of states for the ECLS geometry of Sb:InP(110). In agreement with the *ab initio* phonon calculations by Schmidt and Srivastava[16,17] we have identified up to twelve surface modes involving vibrations of atoms in the adsorbate and the subsurface layers. Some of the calculated surface phonon frequencies are listed in Table III. In general, our results are in good agreement with the recent *ab initio* calculations[18,16,17] and the Raman-scattering experiment.[22] However, the highest A'' phonon mode obtained in this work is nearly 3.0 meV higher than that obtained in the *ab initio* calculations by Fritsch *et al.*[18] and the Raman-scattering experiment,[22] but compares very well with the *ab initio* phonon calculations by Schmidt and Srivastava.[16,17]

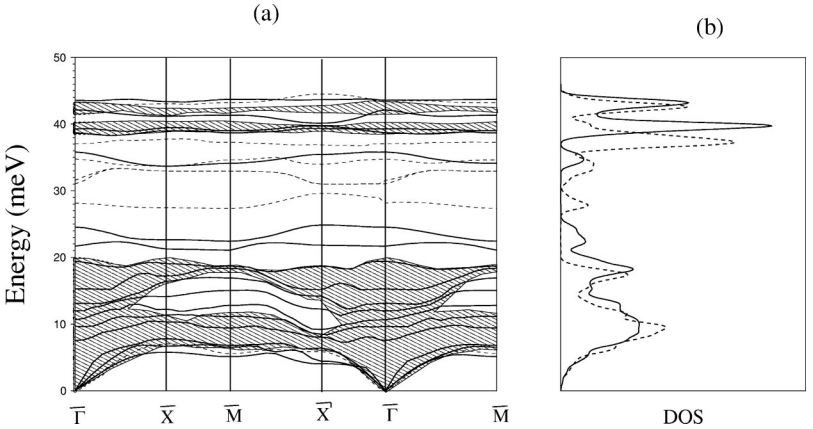

FIG. 9. (a) Phonon-dispersion curves for the epitaxially continued layer structure of Sb:InP(110). The results for the clean InP(110) surface are shown by dashed lines. (b) The corresponding phonon density-of-states curves.

TABLE III. Calculated surface phonon frequencies of Sb:InP(110) for the epitaxial continued structure at the $\bar{\Gamma}$ point and their comparison with recent *ab initio* calculations and a Raman-scattering experiment.

Source	A'' modes				A' modes					
Present	10.5	19.4	39.2	9.7	11.9	19.9	21.6	24.6	35.8	43.5
Raman scattering[a]		20.0	36.0		11.9			22.9	35.8	43.9
ab initio[b]		19.4	35.5		12.6	19.6		23.0	35.9	44.7
ab initio[c]	8.4	19.6	40.3		11.0		20.9	24.0	37.5	47.6

[a]Reference 22.
[b]Reference 18.
[c]Reference 17.

The polarization behavior of all three optical shear A'' modes and the six optical sagittal A' modes are shown in Figs. 10 and 11, respectively. The lowest A'' optical-phonon mode at 10.5 meV results from opposing vibrations of surface- and subsurface-atomic chains in the zigzag chain direction. The second A'' optical mode is totally confined to the adsorbate layer, with vibrations of the neighboring Sb atoms taking place in the zigzag chain direction. The energy of this phonon mode compares very well with that of the Raman-scattering experiment.[22] Similar to the case of As:InP(110), the highest A'' phonon mode is totally localized to the subsurface atoms. Not surprisingly, the energy of this mode is nearly the same for As:InP(110) with both EXS (Fig. 4) and ECLS (Fig. 7) terminations.

The A' mode at 9.7 meV can be described as a rotational mode. We remark that this mode has not been identified in the recent *ab initio* work.[18] The A' mode at 15.9 meV is characterized by opposing motions of the lower Sb atom and the In atom in the second and third layers in the surface normal direction. The phonon mode at 21.5 meV is mainly pictured by opposing motion of surface-layer and subsurface-layer atoms in the [001] direction. Our calculations give two A' phonon modes deep inside the ac-op gap at 24.6 and 35.8 meV. The first one is a bond-stretching mode and mainly results from the opposing motions of the Sb atoms in the [001] direction. A similar displacement pattern has been reported in the work of Fritsch *et al.*[18] for the phonon mode at 23.0 meV. The phonon mode at 35.8 meV compares very well with the phonon modes at 35.9 in the work by Fritsch *et al.*[18] and at 35.8 meV in the Raman-scattering experiment.[22] The Fuchs-Kliewer phonon at 43.5 meV is in very good agreement with the Raman-scattering result at 43.8 meV.[22] This phonon mode is mainly localized on the second-layer P atoms. A similar observation has been made by Fritsch *et al.*[18]

4. Similarities and differences in phonon modes

The results obtained in this work can be used in conjunction with the results obtained by us for clean III-V(110) surfaces using the same theoretical technique, viz., the BCM, to examine similarities and differences in surface phonon modes. We will discuss such features at the $\bar{\Gamma}$ (zone-center)

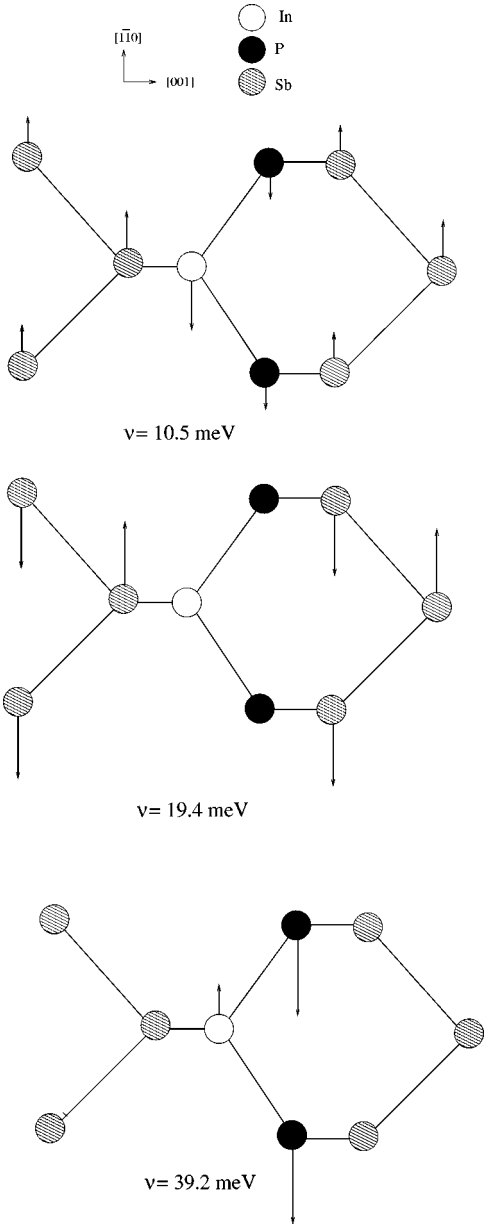

FIG. 10. The atomic displacement patterns of A'' phonon modes for the epitaxially continued layer structure of Sb:InP(110) at the zone center.

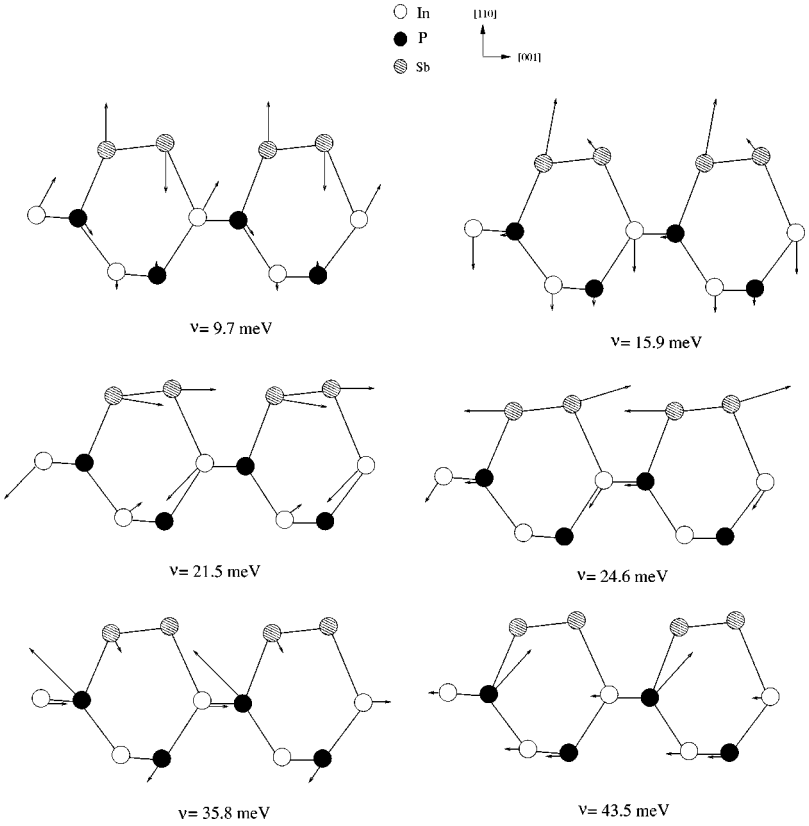

FIG. 11. The atomic displacement patterns of A' phonon modes for the epitaxially continued layer structure of Sb:InP(110) at the zone center.

and $\overline{X'}$ (zone-edge) points, as phonon modes are well characterized at these symmetry points.

a. Zone-center modes. At the $\overline{\Gamma}$ (zone-center) point we are able to make three observations. (i) In our previous works,[31,32] we have reported the presence of a rotational phonon mode on clean III-V(110) and II-VI(110) semiconductor surfaces. This phonon mode mainly involves the vibrations of top-layer atoms. In this work, we have not been able to observe this phonon mode for the adsorption of As, while the corresponding phonon mode is found at 9.7 meV for the adsorption of Sb. The energy location of this phonon mode for the Sb overlayer system is quite close to that for the clean InP(110) surface at 9.1 meV.[31,32] This result is expected for the reason that the energy location of this phonon mode does not depend on the relaxation angle of top-layer atoms. The mode obtained in this work at 9.7 meV compares well with the *ab initio* work of Schmidt and Srivastava[16] who calculated it at 8.4 meV. In general, to our best knowledge, surface modes in this energy range have not been observed in Raman-scattering measurements, probably due to their highly resonant nature.

(ii) For all the considered surface structures in this work, the phonon modes characterized by the motion of subsurface-layer atoms lie at almost the same energy. This can be seen for the highest A'' (see Figs. 4, 7, and 10) and A' (see Figs. 5, 8, and 11) phonon modes. (iii) The highest surface optical-phonon mode can be contributed by atomic displacements in the top three layers, with their relative contributions dependent on their masses. For the clean InP(110)

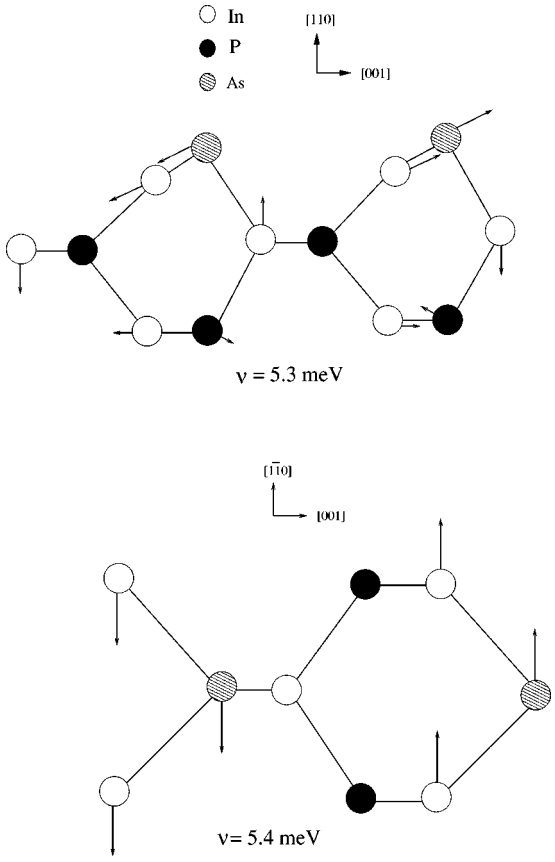

FIG. 12. The surface acoustical phonon frequencies of the exchange-reacted geometry of As:InP(110) at the $\overline{X'}$ point.

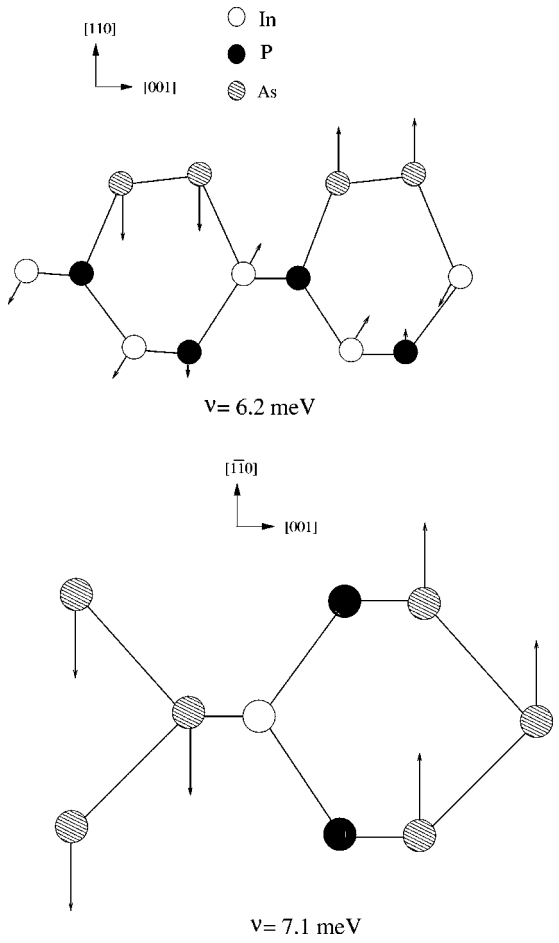

FIG. 13. The surface acoustical phonon frequencies of the epitaxially continued layer structure of As:InP(110) at the $\overline{X'}$ point.

this mode is contributed by atomic vibrations along the $[00\bar{1}]$ direction: top- and second-layer anions vibrating against each other while the top- and second-layer cations vibrating in phase but with smaller amplitude. For the As:InP(110) system with the EXS geometry there is virtually no movement of As atoms, but the anions (P atoms) in the second and third layers vibrate against each other. This pattern is a mixture of those for the clean InP(110) and InAs(110) surfaces.[31,32] It is interesting to compare the vibrational patterns for As:InP(110) with Sb:InP(110) within the ECLS geometry. The vibrational pattern for the ECLS geometry of As:InP(110) is in some sense similar to that for the EXS geometry of As:InP(110) in that there is no movement of the As atom in the anion site, while the As in the cation site vibrates against P in the second layer. In both geometries, the P atoms in the second and third layers vibrate against each other. On the other hand, for the ECLS geometry of Sb:InP(110) there is no movement of (heavy) Sb atoms, and the vibrational pattern is dominated by opposing movements of P atoms in the second and third layers.

b. Zone-edge modes. For all III-V(110) surfaces we have found[31,32] three lowest-surface acoustical frequencies at the zone-edge point $\overline{X'}$ with the A', A'', and A' characters, respectively. However, there are only two surface acoustical phonon frequencies with A' and A'' characters for the adsorption of the As atom. The atomic displacement patterns of these phonon modes are shown in Fig. 12. For the EXS model, the Rayleigh wave (RW) frequency is pictured by the motion of top-layer atoms with components both in the [110] and [001] directions while subsurface-layer In atoms vibrate in the surface normal direction. The vibrational character of this mode is similar to that on the clean InP(110) and InAs(110) surfaces.[31,32] This is due to the similar atomic relaxation pattern of the EXS model and the clean InP(110) and InAs(110) surfaces. However, the vibrational pattern of the RW phonon mode is different for the ECLS model of As:InP(110) (see Fig. 13). For this surface, the top-layer atoms vibrate in the surface normal direction, while the second-layer In atoms have components in both [110] and [001] directions. The second lowest surface acoustic mode is

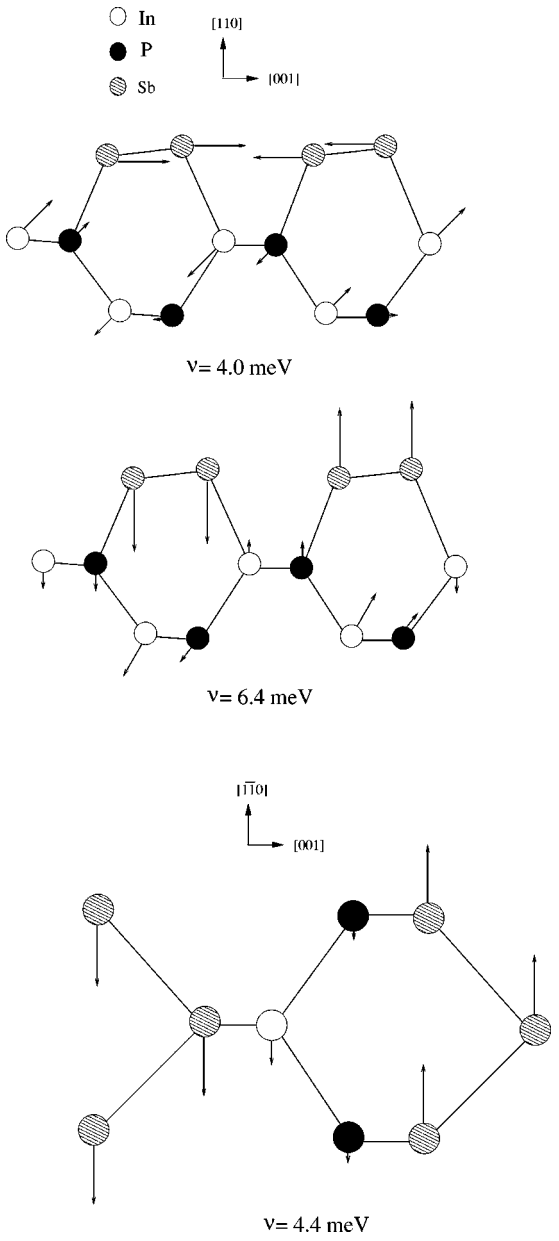

FIG. 14. The surface acoustical phonon frequencies of the epitaxially continued layer structure of Sb:InP(110) at the $\overline{X'}$ point.

a shear mode, strongly localized to the top-layer atoms with their in-phase motion along the zigzag chain. The difference in their energies (5.4 meV for EXS and 7.1 meV for ECLS) is in accordance with the mass difference between In and As atoms, reflecting the difference between the EXS and ECLS geometries.

In contrast to the adsorption of As, there are three acoustical phonon modes with energies 4.0, 4.4, and 6.4 meV at $\overline{X'}$ for the Sb:InP(110) surface. In similarity with clean III-V(110) surfaces,[31,32] the second acoustic mode has A'' polarization while the others have the A' character (see Fig. 14). These phonon modes are mainly localized on the heavy Sb overlayer atoms. The energies, displacement pattern, and polarization of the first two of these modes compare very well with the work by Fritsch *et al.*[18] However, the third surface acoustic mode obtained in the work of Fritsch *et al.* is different from that obtained in this work, because their mode is localized on the second-layer In-P chain and not on the Sb adsorbate layer. Fritsch *et al.* only calculated two acoustic modes localized to the Sb adsorbate layer.

IV. SUMMARY

We have presented *ab initio* calculations of the structural and electronic properties of the EXS and ECLS models of the As:InP(110) surface, based on a plane-wave pseudopotential method within the density-functional theory. In addition to this, the ECLS model of Sb:InP(110) has also been studied. The calculated atomic geometries of all the considered surfaces are in good agreement with recent *ab initio* calculations and experimental findings. Using these atomic geometries and the corresponding charge distribution at surface dangling bonds, we have investigated the full phonon spectrum and density of states for all the considered surfaces using an adiabatic bond-charge model. Our results for the EXS model of As:InP(110) compare well with a recent *ab initio* calculation and Raman-scattering experiment. Furthermore, our results for Sb:InP(110) are found to be in good agreement with the Raman-scattering experiment and recent *ab initio* calculations. The phonon spectra of all considered geometries are compared in detail with that of the clean InP(110) surface. From this comparison we have determined the characteristics of vibrational features due to the adsorption of As and Sb atoms on the InP(110) surface.

First, the deposition of As or Sb on InP(110) results in several characteristic phonon modes in the bulk acoustical-optical gap range. The two geometrical models for As:InP(110) are distinguished from a study of the phonon density of states in the ac-op gap region: the EXS model is characterized by the presence of a clear gap of approximately 10 meV, whereas the ECLS geometry leads to a number of small-peak features. Second, the highest surface phonon frequency for the covered surfaces lies at similar energy to that on the clean InP(110) surface, due to the localization of this phonon mode on the subsurface-layer atoms. Third, due to the large mass of the Sb atom, the Rayleigh vibrational mode on Sb:InP(110) becomes fully localized near the zone boundary $\overline{X'}$, lying well below the acoustic continuum of bulk InP.

[1] P. Skeath, C.Y. Su, W.A. Harrison, I. Lindau, and W.E. Spicer, Phys. Rev. B **27**, 6246 (1983).

[2] C.B. Duke, C. Mailhiot, A. Paton, K. Li, C. Bonapace, and A. Kahn, Surf. Sci. **163**, 391 (1985).

[3] W.K. Ford, T. Guo, D.L. Lessor, and C.B. Duke, Phys. Rev. B **42**, 8952 (1990).

[4] W.K. Ford, T. Guo, K.J. Wan, and C.B. Duke, Phys. Rev. B **45**, 11 896 (1992).

[5] K.E. Miyano, T. Kendelewicz, J.C. Woicik, P.L. Cowan, C.E. Bouldin, B.A. Karlin, P. Pinanetta, and W.E. Spicer, Phys. Rev. B **46**, 6869 (1992).

[6] T. Kendelewicz, J.C. Woicik, K.E. Miyano, A. Herrera-Gomez, P.L. Cowan, B.A. Karlin, C.E. Bouldin, P. Pinanetta, and W.E. Spicer, Phys. Rev. B **46**, 7276 (1992).

[7] C. Nowak, Ph.D. thesis, Berlin University of Technology, 1996.

[8] P. Martensson, G.V. Hansson, M. Lahdeniemi, K.O. Magnusson, S. Wiklund, and J.M. Nicholls, Phys. Rev. B **33**, 7399 (1986).

[9] F. Schaffler, R. Ludeke, A. Taleb-Ibrahimi, G. Hughes, and D. Rieger, J. Vac. Sci. Technol. B **5**, 1048 (1987).

[10] W. Drube and F.J. Himpsel, Phys. Rev. B **37**, 855 (1988).

[11] R.M. Feenstra and P. Martensson, Phys. Rev. Lett. **61**, 447 (1988).

[12] P. Martensson and R.M. Feenstra, Phys. Rev. B **39**, 7744 (1989).

[13] C. Mailhiot, C.B. Duke, and D.J. Chadi, Phys. Rev. B **31**, 2213 (1985).

[14] G.P. Srivastava, Phys. Rev. B **46**, 7300 (1992).

[15] G.P. Srivastava, Surf. Sci. **307**, 328 (1994).

[16] W.G. Schmidt and G.P. Srivastava, Solid State Commun. **89**, 345 (1994).

[17] W.G. Schmidt and G.P. Srivastava, Surf. Sci. **331-333**, 540 (1995).

[18] J. Fritsch, M. Arnold, and U. Schroder, Phys. Rev. B **61**, 16 682 (2000).

[19] U. Grossner, W.G. Schmidt, and F. Bechstedt, Phys. Rev. B **56**, 6719 (1997).

[20] P.V. Santos, B. Koopmans, N. Esser, W.G. Schmidt, and F. Bechstedt, Phys. Rev. Lett. **77**, 759 (1996).

[21] N. Esser, M. Reckzügel, R. Srama, U. Resch, D.R.T. Zahn, W. Richter, C. Stephens, and M. Hünermann, J. Vac. Sci. Technol. B **8**, 680 (1990).

[22] M. Hünermann, L. Geurts, and W. Richter, Phys. Rev. Lett. **66**, 640 (1991).

[23] W. Richter, N. Esser, A. Kelnberger, and M. Köpp, Solid State Commun. **84**, 165 (1992).

[24] N. Esser, M. Köpp, P. Haier, and W. Richter, Phys. Status Solidi A **152**, 191 (1995).

[25] J.P. Perdew and A. Zunger, Phys. Rev. B **23**, 5048 (1981).

[26] G.B. Bachelet, D.R. Hamann, and M. Schlüter, Phys. Rev. B **26**, 4199 (1982).

[27] A. Umerski and G.P. Srivastava, Phys. Rev. B **51**, 2334 (1995).

[28] W. Weber, Phys. Rev. Lett. **33**, 371 (1974).

[29] K.C. Rustagi and W. Weber, Solid State Commun. **18**, 673 (1979).

[30] S.K. Yip and Y.C. Chang, Phys. Rev. B **30**, 7037 (1984).

[31] H.M. Tütüncü and G.P. Srivastava, Phys. Rev. B **53**, 15 675 (1996).
[32] H.M. Tütüncü and G.P. Srivastava, J. Phys. Chem. Solids **58**, 685 (1997).
[33] D.C. Allan and E.J. Mele, Phys. Rev. Lett. **53**, 826 (1984).
[34] A. Mazur and J. Pollmann, Phys. Rev. Lett. **57**, 1811 (1986).
[35] W.G. Schmidt, F. Bechstedt, and G.P. Srivastava, Surf. Sci. Rep. **25**, 141 (1996).
[36] P.H. Borcherds, G.F. Alfrey, D.H. Saunderson, and A.D.B. Woods, J. Phys. C **8**, 2022 (1975).